

Adaptive Control Using Retrospective Cost Optimization with RLS-Based Estimation for Concurrent Markov-Parameter Updating

Mario A. Santillo¹, Matthew S. Holzel², Jesse B. Hoagg³, and Dennis S. Bernstein⁴

Abstract—We present a discrete-time adaptive control law that is effective for systems that are MIMO and either minimum phase or nonminimum phase. The adaptive control algorithm provides guidelines concerning the modeling information needed for implementation. This information includes a sufficient number of Markov parameters to capture the sign of the high-frequency gain as well as the nonminimum-phase zeros. No additional information about the poles or zeros need be known. In this paper, recursive least-squares estimation is used for concurrent Markov parameter estimation. We present numerical examples to illustrate the algorithm’s effectiveness in handling nonminimum-phase zeros as plant changes occur.

I. INTRODUCTION

Adaptive control algorithms can be classified as either direct or indirect, depending on whether they employ an explicit plant parameter estimation algorithm within the overall adaptive scheme; see [1]–[4]. Most direct adaptive control algorithms, with the exception of universal adaptive control algorithms [5], require some prior modeling information, such as the sign of the high-frequency gain. By updating the required modeling information, perhaps through closed-loop identification, a direct adaptive control algorithm can be converted to a hybrid direct and indirect adaptive control algorithm, which may have greater versatility in practice.

The goal of the present paper is to present a hybrid direct and indirect discrete-time adaptive control algorithm as an extension of the direct adaptive control algorithm developed in [6]–[10], demonstrated on the NASA generic transport model in [11], and demonstrated on flow control problems in [12]. This algorithm, based on a retrospective cost optimization (RCO), requires prior estimates of the Markov parameters of the transfer function from the control inputs to the performance variables. These Markov parameter estimates capture the sign of the high-frequency gain as well as the locations of the nonminimum-phase zeros (if any) in the relevant transfer function. Since no parameter estimation is performed online, this algorithm is a direct adaptive control

algorithm. In some applications, however, prior modeling or identification is not possible, whereas, in other applications, the dynamics of the plant may change unexpectedly during operation. In both cases, the required Markov parameters must be estimated online.

The present paper investigates the performance of the RCO-based adaptive control algorithm with concurrent Markov-parameter estimation. The resulting adaptive control algorithm is thus a hybrid direct and indirect algorithm.

For parameter estimation we use a standard recursive least-squares (RLS) algorithm. The scenario we consider uses discrete-time RCO direct adaptive control with prior estimates of the Markov parameters, and the RLS identification algorithm operates concurrently with the control adaptation to update the Markov parameters when a plant change occurs.

We demonstrate the hybrid direct and indirect RCO algorithm on several numerical examples. Of particular interest is the case in which a plant change occurs, in which a minimum phase zero becomes nonminimum phase. These results are noteworthy since nonminimum-phase zeros are known to be challenging for adaptive control algorithms [13]. Numerical results show that the algorithm is able to update the Markov parameters and maintain system stability. These numerical examples are intended to provide motivation for future proofs of stability and convergence.

II. PROBLEM FORMULATION

Consider the MIMO discrete-time system

$$x(k+1) = Ax(k) + Bu(k) + D_1w(k), \quad (1)$$

$$y(k) = Cx(k) + D_2w(k), \quad (2)$$

$$z(k) = E_1x(k) + E_0w(k), \quad (3)$$

where $x(k) \in \mathbb{R}^n$, $y(k) \in \mathbb{R}^{l_y}$, $z(k) \in \mathbb{R}^{l_z}$, $u(k) \in \mathbb{R}^{l_u}$, $w(k) \in \mathbb{R}^{l_w}$, and $k \geq 0$. Our goal is to develop an adaptive output feedback controller under which the performance variable z is minimized in the presence of the exogenous signal w . Note that w can represent either a command signal to be followed, an external disturbance to be rejected, or both. For example, if $D_1 = 0$ and $E_0 \neq 0$, then the objective is to have the output E_1x follow the command signal $-E_0w$. On the other hand, if $D_1 \neq 0$ and $E_0 = 0$, then the objective is to reject the disturbance w from the performance measurement E_1x . The combined command following and disturbance rejection problem is addressed when D_1 and E_0 are block matrices. More precisely, if $D_1 = \begin{bmatrix} \hat{D}_1 & 0 \end{bmatrix}$, $E_0 = \begin{bmatrix} 0 & \hat{E}_0 \end{bmatrix}$, and $w(k) = \begin{bmatrix} w_1(k) \\ w_2(k) \end{bmatrix}$, then

This work was sponsored by NASA under IRAC grant NNX08AB92A and the Department of Defense under a National Defense Science and Engineering Graduate Fellowship.

¹National Defense Science and Engineering Graduate Fellow, Department of Aerospace Engineering, The University of Michigan, Ann Arbor, MI 48109-2140, phone: (734) 764-4319, fax: (734) 763-0578, santillo@umich.edu.

²Graduate Student, Department of Aerospace Engineering, The University of Michigan, Ann Arbor, MI 48109-2140, phone: (734) 615-4406, fax: (734) 763-0578, mholzel@umich.edu.

³Postdoctoral Research Fellow, Department of Aerospace Engineering, The University of Michigan, Ann Arbor, MI 48109-2140, phone: (734) 904-0784, fax: (734) 763-0578, jhoagg@umich.edu.

⁴Professor, Department of Aerospace Engineering, The University of Michigan, Ann Arbor, MI 48109-2140, phone: (734) 764-3719, fax: (734) 763-0578, dsbaero@umich.edu.

the objective is to have E_1x follow the command $-\hat{E}_0w_2$ while rejecting the disturbance w_1 . Lastly, if D_1 and E_0 are empty matrices, then the objective is output stabilization, that is, convergence of z to zero.

Model reference adaptive control (MRAC) is a special case of (1)–(3), where the performance variable z is the difference between the measured output of the plant and the output of the reference model. For MRAC, the exogenous command w is available to the controller as an additional measurement variable, as shown in Figure 1.

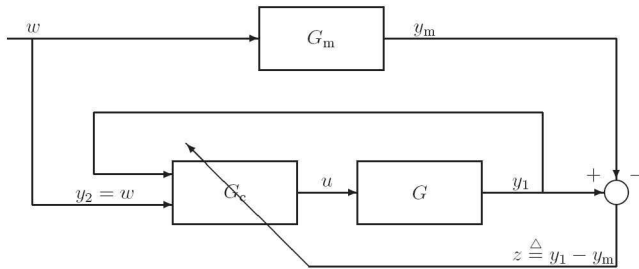


Fig. 1. Model reference adaptive control problem.

III. CONTROLLER CONSTRUCTION

In this section we formulate an adaptive control algorithm for the general control problem represented by (1)–(3). We use a strictly proper time-series controller of order n_c , such that the control $u(k)$ is given by

$$u(k) = \sum_{i=1}^{n_c} M_i(k)u(k-i) + \sum_{i=1}^{n_c} N_i(k)y(k-i), \quad (4)$$

where, for all $i = 1, \dots, n_c$, $M_i \in \mathbb{R}^{l_u \times l_u}$ and $N_i \in \mathbb{R}^{l_u \times l_y}$ are given by the adaptive law presented below. The control can be expressed as

$$u(k) = \theta(k)\phi(k), \quad (5)$$

where

$$\theta(k) \triangleq [N_1(k) \ \dots \ N_{n_c}(k) \ M_1(k) \ \dots \ M_{n_c}(k)],$$

and the regressor vector is given by

$$\phi(k) \triangleq \begin{bmatrix} y(k-1) \\ \vdots \\ y(k-n_c) \\ u(k-1) \\ \vdots \\ u(k-n_c) \end{bmatrix} \in \mathbb{R}^{n_c(l_u+l_y)}. \quad (6)$$

For positive integers p and $p_c \geq p$, we define the extended performance vector $Z(k) \in \mathbb{R}^{p l_z}$, and the extended control vector $U(k) \in \mathbb{R}^{p_c l_u}$ by

$$Z(k) \triangleq \begin{bmatrix} z(k) \\ \vdots \\ z(k-p+1) \end{bmatrix}, \quad U(k) \triangleq \begin{bmatrix} u(k) \\ \vdots \\ u(k-p_c+1) \end{bmatrix}.$$

From (5), it follows that the extended control vector $U(k)$ can be written as

$$U(k) \triangleq \sum_{i=1}^{p_c} L_i \theta(k-i+1) \phi(k-i+1), \quad (7)$$

where

$$L_i \triangleq \begin{bmatrix} 0_{(i-1)l_u \times l_u} \\ I_{l_u} \\ 0_{(p_c-i)l_u \times l_u} \end{bmatrix} \in \mathbb{R}^{p_c l_u \times l_u}. \quad (8)$$

Next, we define the *retrospective performance vector*

$$\hat{Z}(\hat{\theta}, k) \triangleq Z(k) - \bar{B}_{zu} [U(k) - \hat{U}(\hat{\theta}, k)], \quad (9)$$

where $\hat{\theta} \in \mathbb{R}^{l_u \times n_c(l_u+l_y)}$, $\bar{B}_{zu} \in \mathbb{R}^{p l_z \times p_c l_u}$ is given by (25) below, and

$$\hat{U}(\hat{\theta}, k) \triangleq \sum_{i=1}^{p_c} L_i \hat{\theta} \phi(k-i+1). \quad (10)$$

Taking the vec of (9) yields

$$\hat{Z}(\hat{\theta}, k) = f(k) + D(k) \text{vec } \hat{\theta}, \quad (11)$$

where

$$f(k) \triangleq Z(k) - \bar{B}_{zu} U(k), \quad (12)$$

$$D(k) \triangleq \sum_{i=1}^{p_c} \phi^T(k-i+1) \otimes (\bar{B}_{zu} L_i), \quad (13)$$

and \otimes represents the Kronecker product.

Now, consider the retrospective cost function

$$J(\hat{\theta}, k) \triangleq \hat{Z}^T(\hat{\theta}, k) \hat{Z}(\hat{\theta}, k) + \alpha(k) \text{tr} \left[\left(\hat{\theta} - \theta(k) \right)^T \left(\hat{\theta} - \theta(k) \right) \right], \quad (14)$$

where $\alpha(k) > 0$ is the *learning rate*. The learning rate $\alpha(k)$ affects convergence speed of the adaptive control algorithm. As $\alpha(k)$ is increased, convergence speed is lowered. Likewise, as $\alpha(k)$ is decreased, converge speed is raised. Substituting (11) into (14) yields

$$J(\hat{\theta}, k) = c(k) + b^T(k) \text{vec } \hat{\theta} + \left(\text{vec } \hat{\theta} \right)^T A(k) \text{vec } \hat{\theta}, \quad (15)$$

where

$$A(k) = D^T(k)D(k) + \alpha(k)I, \quad (16)$$

$$b(k) = 2D^T(k)f(k) - 2\alpha(k)\text{vec } \theta(k), \quad (17)$$

$$c(k) = f^T(k)f(k) + \alpha(k)\text{tr} [\theta^T(k)\theta(k)]. \quad (18)$$

Since $A(k)$ is positive definite, $J(\hat{\theta}, k)$ has the strict global minimizer $\theta(k+1)$ given by

$$\theta(k+1) = -\frac{1}{2} \text{vec}^{-1} (A^{-1}(k)b(k)). \quad (19)$$

The novel feature of the adaptive control algorithm is the use of the retrospective correction filter (9). This filter provides an inner loop to the adaptive control law by modifying the performance variable $Z(k)$ based on the difference between the actual past control inputs $U(k)$ and

the recomputed past control inputs $\hat{U}(\hat{\theta}, k)$, assuming that the current controller $\hat{\theta}$ had been used in the past.

In the case $z = y$, using the retrospective performance variable $\hat{z}(k) \triangleq [I_{l_z} \ 0_{l_z \times l_z} \ \cdots \ 0_{l_z \times l_z}] \hat{Z}(\theta(k), k)$ in place of y in the regressor vector (6) results in faster convergence.

IV. TIME-SERIES MODELING

The adaptive controller (5) and (19) requires limited model information of the plant (1)–(3); however, the controller does require knowledge of \bar{B}_{zu} . The \bar{B}_{zu} matrix is constructed from the plant's Markov parameters.

Consider the time-series representation of (1)–(3) given by

$$z(k) = \sum_{i=1}^n -\alpha_i z(k-i) + \sum_{i=d}^n \beta_i u(k-i) + \sum_{i=0}^n \gamma_i w(k-i), \quad (20)$$

where $\alpha_1, \dots, \alpha_n \in \mathbb{R}$, $\beta_d, \dots, \beta_n \in \mathbb{R}^{l_z \times l_u}$, $\gamma_0, \dots, \gamma_n \in \mathbb{R}^{l_z \times l_w}$, and the relative degree d is the smallest positive integer i such that the i th Markov parameter $H_i \triangleq E_1 A^{i-1} B$ is nonzero. Note that $\beta_d = H_d$.

Next, consider the μ -MARKOV model of (20) obtained from μ successive back-substitutions of (20) into itself, and given by

$$\begin{aligned} z(k) = & - \sum_{i=1}^n \alpha_{\mu,i} z(k-\mu-i) + \sum_{i=d}^{\mu} H_{zu,i} u(k-i) \\ & + \sum_{i=1}^n \beta_{\mu,i} u(k-\mu-i) + \sum_{i=0}^{\mu} H_{zw,i} w(k-i) \\ & + \sum_{i=1}^n \gamma_{\mu,i} w(k-\mu-i), \end{aligned} \quad (21)$$

where $\alpha_{\mu,i} \in \mathbb{R}$, $\beta_{\mu,i} \in \mathbb{R}^{l_z \times l_u}$, $\gamma_{\mu,i} \in \mathbb{R}^{l_z \times l_w}$, $H_{zu,i} \in \mathbb{R}^{l_z \times l_u}$, $H_{zw,i} \in \mathbb{R}^{l_z \times l_w}$, and $\mu \geq d$. Thus, the μ -MARKOV transfer function from u to z is given by

$$\begin{aligned} G_{\mu, zu}(\mathbf{z}) = & \frac{1}{p_{\mu}(\mathbf{z})} (H_d \mathbf{z}^{\mu+n-d} + \cdots + H_{\mu} \mathbf{z}^n) \\ & + \frac{1}{p_{\mu}(\mathbf{z})} (\beta_{\mu,1} \mathbf{z}^{n-1} + \cdots + \beta_{\mu,n}), \end{aligned} \quad (22)$$

where $p_{\mu}(\mathbf{z}) \triangleq \mathbf{z}^{\mu+n} + \alpha_{\mu,1} \mathbf{z}^{n-1} + \cdots + \alpha_{\mu,n}$. This system representation is nonminimal, overparameterized, and has order $n + \mu$. Note that the coefficients of the terms $\mathbf{z}^{n+\mu-1}$ through \mathbf{z}^n in the denominator are zero.

The Laurent series expansion of $G_{zu}(\mathbf{z})$ about $\mathbf{z} = \infty$ is

$$G_{zu}(\mathbf{z}) = \sum_{i=d}^{\infty} \mathbf{z}^{-i} H_{zu,i}. \quad (23)$$

Truncating the numerator and denominator of (22) is equivalent to the truncated Laurent series expansion of $G_{zu}(\mathbf{z})$ about $\mathbf{z} = \infty$. Thus, the truncated Laurent series expansion of $G_{zu}(\mathbf{z})$ is

$$\bar{G}_{\mu, zu}(\mathbf{z}) \triangleq \sum_{i=d}^{\mu} \mathbf{z}^{-i} H_{zu,i}. \quad (24)$$

Next, define $p_c \triangleq p + \mu$ and the resulting block-Toeplitz control matrix $\bar{B}_{zu} \in \mathbb{R}^{p_c l_z \times p_c l_u}$ is

$$\bar{B}_{zu} \triangleq \begin{bmatrix} 0_{l_z \times d l_u} & H_{zu,d} & \cdots & H_{zu,\mu} & 0_{l_z \times l_u(p-1)} \\ \vdots & & \ddots & \vdots & \\ 0_{l_z \times d l_u} & 0_{l_z \times l_u(p-1)} & H_{zu,d} & \cdots & H_{zu,\mu} \end{bmatrix}. \quad (25)$$

The leading zeros in the first row of \bar{B}_{zu} account for the nonzero relative degree d . The advantage in constructing \bar{B}_{zu} using the Markov parameters $H_{zu,d}, \dots, H_{zu,\mu}$ as opposed to using all of the numerator coefficients of $G_{\mu, zu}$ is ease of identification.

Note that for a single-input, single-output system, some of the roots of the polynomial

$$\begin{aligned} H(\mathbf{z}) \triangleq & H_{zu,d} \mathbf{z}^{\mu-d} + H_{zu,d+1} \mathbf{z}^{\mu-d-1} + \cdots + H_{zu,\mu-1} \mathbf{z} \\ & + H_{zu,\mu} \end{aligned} \quad (26)$$

can be shown to approximate the nonminimum-phase zeros from u to z that lie outside of a circle in the complex plane centered at the origin with radius equal to the spectral radius of A . Thus, knowledge of $H_{zu,d}, \dots, H_{zu,\mu}$ encompasses knowledge of the nonminimum-phase zeros from u to z that lie outside of the spectral radius of A . In fact, if the transfer function from u to z is minimum phase, then we choose $\mu = d$, which requires knowledge of only a single Markov parameter, namely, H_d . The minimum-phase case with $z = y$ is considered in [8] using a gradient-based adaptive law rather than the adaptive law (19). Under the minimum-phase assumption, [8] proves asymptotic convergence of z to zero.

V. RECURSIVE LEAST-SQUARES MARKOV PARAMETER UPDATE

To obtain the required Markov parameters for constructing \bar{B}_{zu} , we implement the standard recursive least-squares (RLS) algorithm as in [14] for the μ -MARKOV plant structure (21). We initialize the parameter matrix to zero and the covariance matrix of the parameter estimation error to the identity matrix. At each time step, we take the computed Markov parameters H_i , $i = 0, \dots, \mu$, and construct \bar{B}_{zu} as in (25). The identification input for RLS is taken to be the output of the adaptive controller, that is, the control input u to the plant, while the identification output for RLS is taken to be the performance variable z . The closed-loop system including the RCO adaptive control algorithm with concurrent RLS identification for Markov parameter, and thus \bar{B}_{zu} , updates is shown in Figure 2. No probing input is used to identify the Markov parameters, and disturbances are assumed to be present while the online identification takes place.

VI. NUMERICAL EXAMPLES

We now present numerical examples to illustrate the response of the RCO adaptive control algorithm with concurrent RLS identification. We consider a sequence of examples with increasing complexity. In each case, we start with a nominal plant in closed loop with the RCO adaptive control

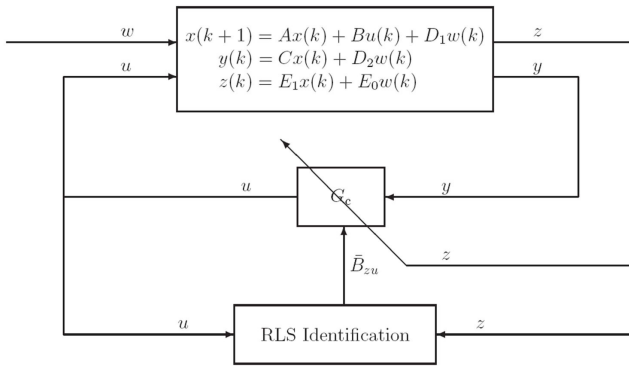


Fig. 2. Closed-loop system including the RCO adaptive control algorithm with concurrent RLS identification for Markov parameter updates.

algorithm and concurrent RLS identification. At some time during the simulation, a plant change occurs, which requires updating the Markov parameters for the adaptive controller. As RLS identification runs concurrently with the adaptive controller, the Markov parameters are updated in real time. Each plant can be viewed as a sampled-data discretization of a continuous-time plant sampled at $T_s = 0.01$ sec. All examples assume $z = y$.

Each example, unless otherwise noted, is a disturbance rejection problem, that is, $E_0 = 0$, with unknown sinusoidal disturbance given by

$$w(k) = \begin{bmatrix} \sin 2\pi\nu_1 kT_s \\ \sin 2\pi\nu_2 kT_s \end{bmatrix}, \quad (27)$$

where $\nu_1 = 5$ Hz and $\nu_2 = 13$ Hz. The RCO adaptive control algorithm requires no information about w . With each plant realized in controllable canonical form, we take $D_1 = \begin{bmatrix} I_2 \\ 0 \end{bmatrix}$, and, therefore, the disturbance is not matched.

A. Example: Change in control effectiveness

Consider a stable, minimum-phase, SISO plant with poles $0.5 \pm 0.5j$, $-0.5 \pm 0.5j$, ± 0.9 , and $\pm 0.7j$; and zeros $0.3 \pm 0.7j$, $-0.7 \pm 0.3j$, and ± 0.5 . Let $n_c = 15$, $p = 1$, $\mu = 3$, and $\alpha = 25$. The closed-loop response is shown in Figure 3. The control is turned on at $t = 5$ sec, and the performance variable reduces to zero. At $t = 15$ sec, the system suffers a 75% loss of control effectiveness, that is, the control input u entering the plant is multiplied by a scaling factor $\lambda = 0.25$. The Markov parameters are updated online, and the performance variable reduces to zero. Figure 4 shows a time-history plot of the first 3 Markov parameters obtained from online RLS identification.

B. Example: Change in zero characteristics

Consider a stable, minimum-phase, SISO plant with poles $0.5 \pm 0.5j$, $-0.5 \pm 0.5j$, ± 0.9 , and $\pm 0.7j$; and zeros $0.3 \pm 0.7j$, $-0.7 \pm 0.3j$, and ± 0.5 . Let $n_c = 20$, $p = 1$, $\mu = 20$, and $\alpha = 1000$. The closed-loop response is shown in Figure 5. The control is turned on at $t = 5$ sec, and the performance variable reduces to zero. At $t = 15$ sec, the minimum-phase zero at $\mathbf{z} = 0.5$ is changed to a nonminimum-phase zero

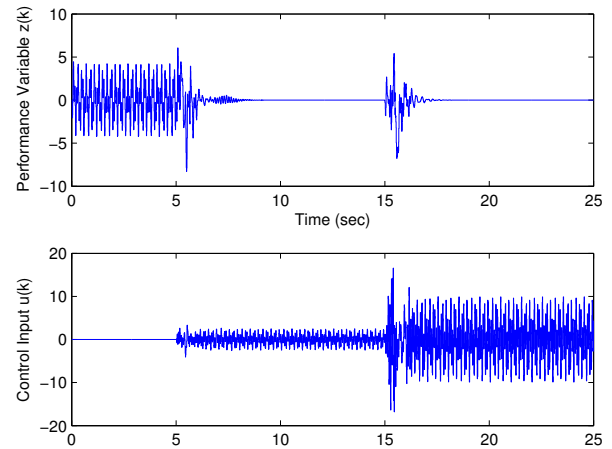


Fig. 3. Closed-loop disturbance rejection response for a stable, minimum-phase, SISO plant. The control is turned on at $t = 5$ sec, and, at $t = 15$ sec, the system suffers a 75% loss of control effectiveness. The controller order is $n_c = 15$ with parameters $p = 1$, $\mu = 3$, $\alpha = 25$.

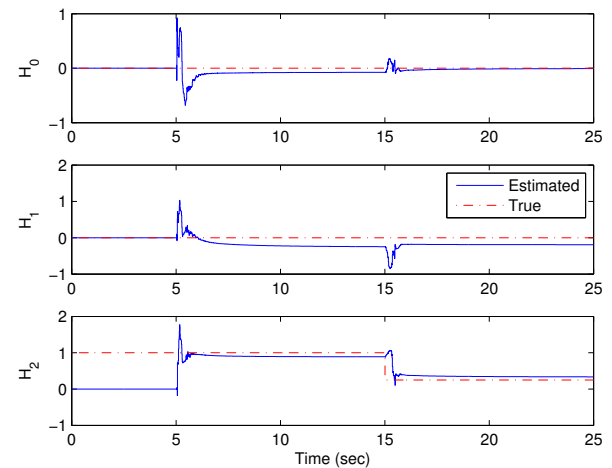


Fig. 4. Time history of the first 3 Markov parameters obtained from online RLS identification. The control is turned on at $t = 5$ sec, and, at $t = 15$ sec, the system suffers a 75% loss of control effectiveness. The estimated Markov parameters are used in the adaptive controller update law.

at $\mathbf{z} = 2$. After a transient, the adaptive control algorithm reduces the performance variable to zero.

C. Example: Change in poles and zeros

Consider an order $n = 8$ FIR, nonminimum-phase, SISO plant with zeros $0.3 \pm 0.7j$, $-0.7 \pm 0.3j$, 0.5 , and 2 . Let $n_c = 15$, $p = 1$, $\mu = 10$, and $\alpha = 25$. The closed-loop response is shown in Figure 6. The control is turned on at $t = 5$ sec, and the performance variable reduces to zero. At $t = 15$ sec, the nonminimum-phase zero at $\mathbf{z} = 2$ is changed to a minimum-phase zero at $\mathbf{z} = 0.5$ and the plant's poles are changed to $0.5 \pm 0.5j$, $-0.5 \pm 0.5j$, and $\pm 0.7j$. After a transient, the adaptive control algorithm reduces the performance variable to zero.

D. Example: Change in relative degree

Consider a stable, nonminimum-phase, SISO plant with poles $0.5 \pm 0.5j$, $-0.5 \pm 0.5j$, ± 0.9 , and $\pm 0.7j$; and zeros $0.3 \pm 0.7j$, $-0.7 \pm 0.3j$, 0.5 , and 2 . Let $n_c = 15$, $p = 2$,

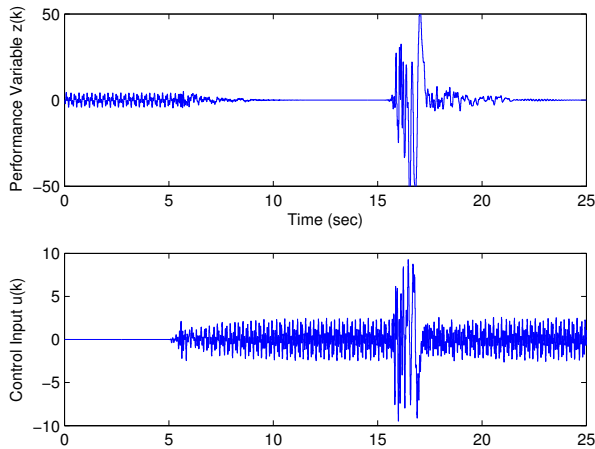


Fig. 5. Closed-loop disturbance rejection response for a stable, minimum-phase, SISO plant. The control is turned on at $t = 5$ sec, and, at $t = 15$ sec, one of the plant's minimum-phase zeros is replaced with a nonminimum-phase zero. The controller order is $n_c = 20$ with parameters $p = 1, \mu = 20, \alpha = 1000$.

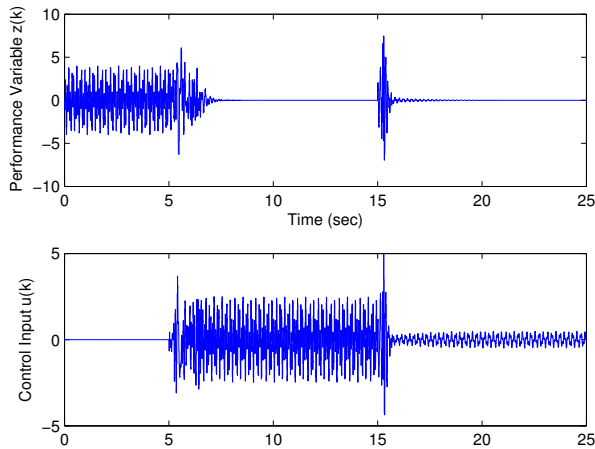


Fig. 6. Closed-loop disturbance rejection response for an FIR, nonminimum-phase, SISO plant. The control is turned on at $t = 5$ sec, and, at $t = 15$ sec, the plant's nonminimum-phase zero is replaced with a minimum-phase zero and the plant's poles are relocated to stable poles away from the origin. The controller order is $n_c = 15$ with parameters $p = 1, \mu = 10, \alpha = 25$.

$\mu = 10$, and $\alpha = 50$. The closed-loop response is shown in Figure 7. The control is turned on at $t = 5$ sec, and the performance variable reduces to zero. At $t = 15$ sec, the plant's relative degree is changed from $d = 2$ to $d = 4$ by adding two poles at the origin. The RLS algorithm identifies the shifted Markov parameters due to the latency and recovers performance. Without RLS, the RCO algorithm is shown in [9] to be sensitive to unknown delays.

E. Example: Command following with change in zeros

We now consider a step-command following problem with command given by a square wave of frequency $2\pi\nu_3 T_s$ where $\nu_3 = 0.1$ Hz. With the plant realized in controllable canonical form, we take $D_1 = 0$ and $E_0 = -1$.

Consider a stable, nonminimum-phase, SISO plant with poles $0.5 \pm 0.5j$, $-0.5 \pm 0.5j$, ± 0.9 , and $\pm 0.7j$; and zeros $0.3 \pm 0.7j$, $-0.7 \pm 0.3j$, 0.5 , and 2 . Let $n_c = 15$, $p = 2$,

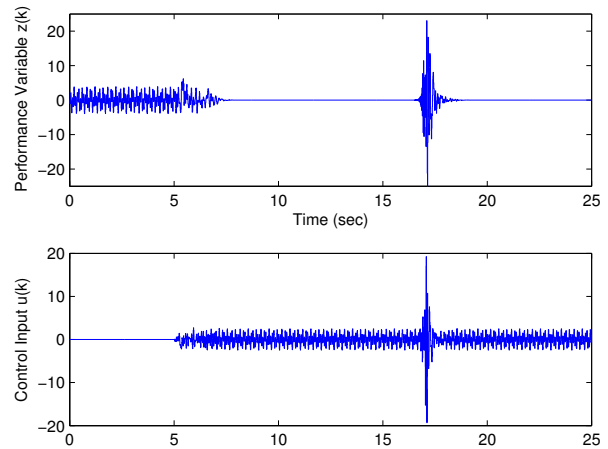


Fig. 7. Closed-loop disturbance rejection response for a stable, nonminimum-phase, SISO plant. The control is turned on at $t = 5$ sec, and, at $t = 15$ sec, the plant's relative degree changes from $d = 2$ to $d = 4$. The controller order is $n_c = 15$ with parameters $p = 2, \mu = 10, \alpha = 50$.

$\mu = 25$, and $\alpha = 250$. The closed-loop response is shown in Figure 8. The control is turned on at $t = 5$ sec, and the performance variable reduces to zero. At $t = 15$ sec, the minimum-phase zero at $z = 0.5$ disappears from the plant, while the nonminimum-phase zero at $z = 2$ is changed to a nonminimum-phase zero at $z = 2.5$. After a transient, the adaptive control algorithm reduces the performance variable to zero and follows the step command.

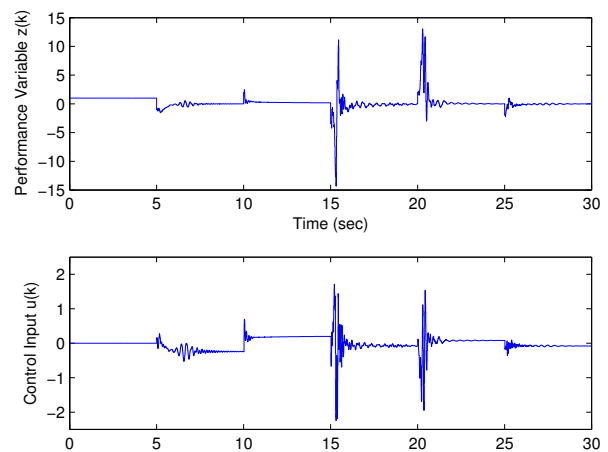


Fig. 8. Closed-loop command following response for a stable, nonminimum-phase, SISO plant. The control is turned on at $t = 5$ sec, and, at $t = 15$ sec, one of the plant's minimum-phase zeros is removed while the location of the plant's nonminimum-phase zero is changed. The controller order is $n_c = 15$ with parameters $p = 2, \mu = 25, \alpha = 250$.

F. Example: MRAC for Missile Longitudinal Dynamics

We now present a numerical example for MRAC of missile longitudinal dynamics under an off-nominal or damage situation. The MRAC control architecture is shown in Figure 1. The basic missile longitudinal plant of [15] is derived from the short period approximation of the longitudinal equations

of motion, given by

$$\dot{x} = \begin{bmatrix} -1.064 & 1 \\ 290.26 & 0 \end{bmatrix} x + \lambda \begin{bmatrix} -0.25 \\ -331.4 \end{bmatrix} u, \quad (28)$$

$$y = \begin{bmatrix} -123.34 & 0 \\ 0 & 1 \end{bmatrix} x + \lambda \begin{bmatrix} -13.51 \\ 0 \end{bmatrix} u, \quad (29)$$

where

$$x \triangleq \begin{bmatrix} \alpha \\ q \end{bmatrix}, \quad y \triangleq \begin{bmatrix} A_z \\ q \end{bmatrix},$$

and $\lambda \in (0, 1]$ represents the control effectiveness. Nominally $\lambda = 1$.

The open-loop system (28), (29) is statically unstable. To overcome this instability, a classical three-loop autopilot from [15] is wrapped around the basic missile longitudinal plant. The adaptive controller then augments the closed-loop system to provide control in off-nominal cases, that is, when $\lambda < 1$. The autopilot and adaptive controller inputs are denoted u_{ap} and u_{ac} , respectively. Thus, the total control input $u = u_{ap} + u_{ac}$. The reference model G_m consists of the basic missile longitudinal plant with $\lambda = 1$ and the classical three-loop autopilot. An actuator saturation of ± 30 deg is included in the model, but no actuator or sensor dynamics are included.

Our goal is to have the missile follow a pitch acceleration command w consisting of a 1-g amplitude, 1-Hz square wave. The performance variable z is the difference between the measured pitch acceleration A_z and the reference model pitch acceleration A_z^* , that is, $z \triangleq A_z - A_z^*$. The adaptive controller is implemented at a sampling rate of 300 Hz. We take $n_c = 3$, $p = 1$, and $\mu = 20$. A time-varying learning rate α is used such that, initially, controller adaptation is fast, and, as performance improves, the adaptation slows.

Figure 9 shows closed-loop MRAC simulation results. Initially, $\lambda = 1$, and thus, the adaptive controller is not used. At $t = 5$ sec, we change $\lambda = 0.5$, but, to demonstrate autopilot-only control, we do not turn on the adaptive controller. At $t = 10$ sec, the adaptive controller is turned on. After a transient, the augmented controllers result in better performance than the autopilot-only control.

VII. CONCLUSION

We presented a hybrid direct and indirect RCO adaptive control algorithm and demonstrated its effectiveness through numerical examples. The adaptive control algorithm requires a sufficient number of Markov parameters to capture the sign of the high-frequency gain as well as the nonminimum-phase zeros. No additional information about the poles or zeros need be known. Recursive least-squares estimation was used for concurrent Markov parameter updating. Future work includes the development of Lyapunov-based stability and robustness analysis for the RCO adaptive control algorithm.

REFERENCES

- [1] G. C. Goodwin and K. S. Sin, *Adaptive Filtering, Prediction, and Control*. Prentice Hall, 1984.
- [2] K. S. Narendra and A. M. Annaswamy, *Stable Adaptive Systems*. Englewood Cliffs, New Jersey: Prentice Hall, 1989.
- [3] P. Ioannou and J. Sun, *Robust Adaptive Control*. Prentice Hall, 1996.

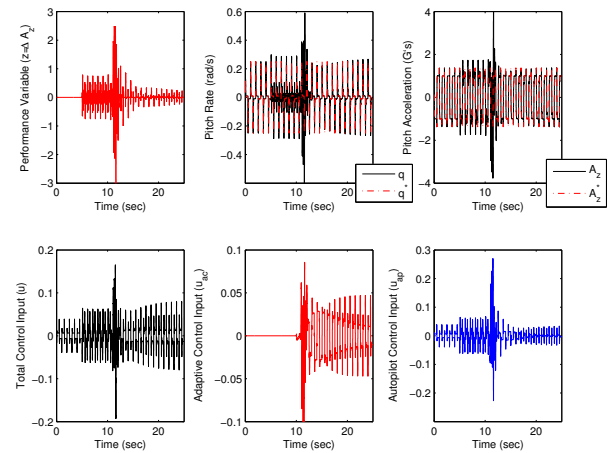


Fig. 9. Closed-loop model reference adaptive control of missile longitudinal dynamics. Initially, $\lambda = 1$. At $t = 5$ sec, we change $\lambda = 0.5$ but the adaptive controller remains off. At $t = 10$ sec, the adaptive controller is turned on. After a transient, the augmented controllers result in better performance than the autopilot-only control.

- [4] I. Mareels and J. W. Polderman, *Adaptive Systems: An Introduction*. Boston, MA: Birkhäuser, 1996.
- [5] A. Ilchmann, *Non-Identifier-Based High-Gain Adaptive Control*. London, England: Springer-Verlag, 1993.
- [6] R. Venugopal and D. S. Bernstein, "Adaptive disturbance rejection using ARMARKOV/Toeplitz models," *IEEE Trans. Contr. Sys. Tech.*, vol. 8, pp. 257–269, 2000.
- [7] H. R. Sane, R. Venugopal, and D. S. Bernstein, "Disturbance rejection using ARMARKOV adaptive control with simultaneous identification," *IEEE Trans. Contr. Sys. Tech.*, vol. 9, pp. 101–106, 2001.
- [8] J. B. Hoagg, M. A. Santillo, and D. S. Bernstein, "Discrete-time adaptive command following and disturbance rejection with unknown exogenous dynamics," *IEEE Trans. Autom. Contr.*, vol. 53, pp. 912–928, 2008.
- [9] M. A. Santillo and D. S. Bernstein, "Inherent robustness of minimal modeling discrete-time adaptive control to flight anomalies," in *Proc. Guid. Nav. Contr. Conf.*, Honolulu, HI, August 2008, AIAA-2008-7289.
- [10] —, "A retrospective correction filter for discrete-time adaptive control of nonminimum phase systems," in *Proc. Conf. Dec. Contr.*, Cancun, Mexico, December 2008, pp. 690–695.
- [11] M. S. Holzel, M. A. Santillo, J. B. Hoagg, and D. S. Bernstein, "Adaptive control of the NASA generic transport model using retrospective cost optimization," in *Proc. AIAA Guid. Nav. Contr. Conf.*, August 2009, AIAA-2009-5616.
- [12] M. S. Flederjohn, Y.-C. Cho, J. B. Hoagg, M. A. Santillo, W. Shyy, and D. S. Bernstein, "Retrospective cost adaptive flow control using a dielectric barrier discharge actuator," in *Proc. AIAA Guid. Nav. Contr. Conf.*, August 2009, AIAA-2009-5857.
- [13] B. Anderson, "Topical problems of adaptive control," in *Proc. European Contr. Conf.*, Kos, Greece, July 2007, pp. 4997–4998.
- [14] L. Ljung, *System Identification: Theory for the User, 2nd ed.* Upper Saddle River, NJ: Prentice-Hall Information and Systems Sciences, 1999.
- [15] C. Mracek and D. Ridgely, "Missile longitudinal autopilots: Connections between optimal control and classical topologies," in *AIAA Guidance, Navigation, and Control Conference and Exhibit*, San Francisco, CA, Aug. 15–18, 2005, AIAA-2005-6381.